Forced Spaser Oscillations

Alexander A. Lisyansky[a], Eugeny S. Andrianov[b], Alexander V. Dorofeenko[b], Alexander A. Pukhov[b], and Alexey P. Vinogradov[b]

[a]Dept. of Physics, Queens College of the City University of New York, Flushing, NY, USA 11367
[b]Institute for Theoretical and Applied Electromagnetics, 13 Izhorskaya, Moscow, Russia 125412

ABSTRACT

We study oscillations of a spaser driven by an external optical wave. When the frequency of the external field is shifted from the frequency of an autonomous spaser, the spaser exhibits stochastic oscillations at low field intensity. The plasmon oscillations lock to the frequency of the external field only when the field amplitude exceeds a threshold value. We find a region of external field amplitude and the frequency detuning (the Arnold tongue) for which the spaser becomes synchronized with the external wave. We obtain the conditions upon the amplitude and frequency of the external field (the curve of compensation) at which the spaser's dipole moment oscillates with a phase shift of π relatively to the external wave. For these values of the amplitude and frequency, the loss in the metal nanoparticles within the spaser is exactly compensated for by the gain. It is expected that if these conditions are not satisfied, then due to loss or gain of energy, the amplitude of the wave travelling along the system of spasers either tends to the curve of compensation or leave the Arnold tongue. We also consider cooperative phenomena showing that in a chain of interacting spasers, depending on the values of the coupling constants, either all spasers oscillate in phase or a nonlinear autowave travels in the system. In the latter scenario, the traveling wave is harmonic, unlike excitations in other nonlinear systems. Due to the nonlinear nature of the system, any initial distribution of spaser states evolves into one of these steady states.

Keywords: spaser, synchronization, loss compensation, Arnold tongue, spaser chain

1. INTRODUCTION

Artificially created composite structures – plasmonic metamaterials – attract ever-growing interest thanks to their perspectives of having properties not readily available in nature[1,2]. Numerous applications of metamaterials containing metallic nanoparticles (NPs) cannot be realized due to the high level of Joule losses. In particular, the near field harmonics excited on the surface of metamaterial can create a perfect image[3]. Energy loss in metamaterials causes the energy transfer by the near fields resulting in a phase difference between "interfering" evanescent harmonics[4]. The dephasing of these harmonics results in their destructive interference and degrading of the perfect image[5]. To compensate for losses, gain media (atoms, molecules or quantum dots) can be included into the matrix of metamaterial[6-11]. However, not only dissipation but also amplification, which is also connected with the energy flux and dephasing, destroys a perfect image. Therefore, one needs an exact compensation of losses.

When gain medium is introduced into a metamaterial, a combination of a nanoscale active medium having the population inversion with a metal NP results in the emergence of a nanoplasmonic counterpart of the laser – surface plasmon amplification by stimulated emission of radiation (spaser) first proposed by Bergman and Stockman[12] and realized experimentally by Noginov at al.[13] Below, to be specific, we consider quantum dots (QDs) as gain particles. In this context, the spaser is a plasmonic nanoparticle NP surrounded with QDs[12,14]. It is implied that the inverse population of a QD is due to an external incoherent pumping.

The principles of operation of the spaser are analogous to those for the laser with the role of photons played by surface plasmons (SPs) localized at a NP[12,14]. SPs are confined to a NP, which resembles a resonator. The spaser generates and amplifies the near field of the NP. The SP amplification occurs due to the nonradiative energy transfer from QDs to the NP. This process originates from the dipole-dipole (or any other near field[15]) interaction between QDs and the plasmonic NP. This physical mechanism has high efficiency because the probability of exciting the SP is greater than the probability of radiative emission by a factor of $\sim (k_0 r)^{-3}$, where r is the distance between the centers of the NP and a QD and k_0 is an optical wavenumber in vacuum[16]. Stimulated radiation from QDs into the plasmon mode results in spasing.

Thus, plasmonic mode is excited by pumping QDs. This process is inhibited by losses in the NP, which together with pumping results in undamped stationary oscillations of the spaser dipole moment.

When spasers are used as plasmonic inclusions forming a gain metamaterial, the oscillations of their dipole moments are caused not only by the external field but also by the fields produced by QDs, which actually tends to compensate for loss. However, even in the absence of an external field, a spaser operating above the pumping threshold D_{th} (the spasing regime) is an autonomic (self-oscillating) system exhibiting undamped harmonic oscillations of the dipole moment. These oscillations are characterized by their own frequency and amplitude depending on pumping. The autonomic frequency of this self-oscillation is determined by the plasmon frequency, transition frequency of the gain inclusion and characteristic times of relaxation in the NP and excitation of gain inclusions[17]. Therefore, in order to develop a correct description of metamaterials with spasers, it is necessary to study the interaction of the spaser with the external field in details.

In this communication, we study analytically and numerically the operation of a spaser driven by an external optical wave above and below the pumping threshold. We demonstrate that the pumping drastically changes the spaser's behavior in the optical field in comparison with the behavior of a passive QD-NP pair. In particular, when the frequency of the external field is detuned from the autonomic frequency of the spaser, even infinitesimally weak field may drive the spaser to stochastic oscillations. For the spasing regime, we find a region of values of the external field amplitude and the frequency detuning (the Arnold tongue) for which the spaser synchronizes with the external wave. We show that for both above and below pumping threshold regimes, there is a relationship between the amplitude and frequency of the field at which the NP dipole moment oscillates with the phase shift of π relatively to the external wave, so that losses at the NP are exactly compensated by gain.

2. EQUATIONS OF MOTIONS FOR A SPASER

We consider a simplest model of spaser as a two level QD of size r_{TLS} placed near a plasmonic spherical NP of size r_{NP}[12]. The energy from the pumped QD is radiationless transferred to the NP exciting SPs. At the frequency of the SP resonance ω_{SP}, the dynamics of the NP polarization is governed by the oscillator equation

$$\ddot{\mathbf{d}}_{NP} + \omega_{SP}^2 \mathbf{d}_{NP} = 0. \tag{1}$$

The quantization of this oscillator can be performed in an ordinary way by introducing the Bose operators $\hat{\bar{a}}^{\dagger}(t)$ and $\hat{\bar{a}}(t)$ for the creation and annihilation of the dipole SP[18]:

$$\hat{\mathbf{d}}_{NP} = \boldsymbol{\mu}_{NP} \left(\hat{\bar{a}} + \hat{\bar{a}}^{\dagger} \right). \tag{2}$$

The corresponding Hamiltonian is

$$\hat{H}_{SP} = \frac{\hbar \omega_{SP}}{2} \left(\hat{\bar{a}}^{\dagger} \hat{\bar{a}} + \hat{\bar{a}} \hat{\bar{a}}^{\dagger} \right). \tag{3}$$

To determine the value $\boldsymbol{\mu}_{NP}$, we should compare Hamiltonians of a single plasmon and the quant

$$\frac{\hbar \omega_{SP}}{2} \left(\hat{\bar{a}}^{\dagger} \hat{\bar{a}} + \hat{\bar{a}} \hat{\bar{a}}^{\dagger} \right) = \frac{1}{8\pi} \int_{\substack{volume \\ of\ NP}} \omega \frac{\partial \operatorname{Re} \varepsilon_{NP}(\omega)}{\partial \omega} \bigg|_{\omega_{SP}} \hat{\mathbf{E}}_i \cdot \hat{\mathbf{E}}_i^{\dagger} dV, \tag{4}$$

where ε_{NP} and $\hat{\mathbf{E}}_i$ are the permittivity and the electric field operator inside the NP, respectively. For a spherical NP, the electric field of the SP is connected with the dipole moment operator as $\hat{\mathbf{E}}_i = -\hat{\mathbf{d}}_{NP} r_{NP}^{-3} = -\boldsymbol{\mu}_{NP} r_{NP}^{-3} \left(\hat{\bar{a}} + \hat{\bar{a}}^{\dagger} \right)$ inside of the NP. Substituting the latter expression into Eq. (4) and eliminating the terms $\hat{\bar{a}}\hat{\bar{a}}$ and $\hat{\bar{a}}^{\dagger}\hat{\bar{a}}^{\dagger}$ in the rotating wave approximation, we get

$$\frac{\hbar\omega_{SP}}{2} = \frac{|\mathbf{\mu}_{NP}|^2}{6r_{NP}^3}\omega_{SP}\left.\frac{\partial\operatorname{Re}\varepsilon_{NP}(\omega)}{\partial\omega}\right|_{\omega_{SP}}. \tag{5}$$

Finally, we obtain

$$\mathbf{\mu}_{NP}^2 = 3\hbar r_{NP}^3 \Bigg/ \left.\left(\frac{\partial\operatorname{Re}\varepsilon_{NP}(\omega)}{\partial\omega}\right)\right|_{\omega_{SP}} \tag{6}$$

The quantum description of a two-level QD is done via the transition operator $\hat{\bar{\sigma}} = |g\rangle\langle e|$ between excited $|e\rangle$ and ground $|g\rangle$ states of the QD, so that the operator for the dipole moment of the QD is represented as

$$\hat{\mathbf{\mu}}_{TLS} = \mathbf{\mu}_{TLS}\left(\hat{\bar{\sigma}}(t) + \hat{\bar{\sigma}}^\dagger(t)\right), \tag{7}$$

where $\mathbf{\mu}_{TLS} = \langle e|e\mathbf{r}|g\rangle$ is the QD dipole moment matrix element. The Hamiltonian of the two-level QD can be written as

$$\hat{H}_{TLS} = \hbar\omega_{TLS}\hat{\bar{\sigma}}^\dagger\hat{\bar{\sigma}}, \tag{8}$$

where ω_{TLS} is the transition frequency of the QD. The commutation relations for operators $\hat{\bar{a}}(t)$ and $\hat{\bar{\sigma}}(t)$ are standard: $\left[\hat{\bar{a}}(t),\hat{\bar{a}}^+(t)\right] = 1$ and $\left[\hat{\sigma}^\dagger,\hat{\sigma}\right] = \hat{D}$, where the operator $\hat{D} = \left[\hat{\sigma}^\dagger,\hat{\sigma}\right] = \hat{n}_e - \hat{n}_g$ describes the population inversion of the ground $\hat{n}_g = |g\rangle\langle g|$ and excited states $\hat{n}_e = |e\rangle\langle e|$, $\hat{n}_g + \hat{n}_e = \hat{1}$, of the QD.

We describe the dynamics of the free spaser by the model Hamiltonian[11,12,19]

$$\hat{H} = \hat{H}_{SP} + \hat{H}_{TLS} + \hat{V} + \hat{\Gamma}, \tag{9}$$

where the operator

$$\hat{V} = -\hat{\mathbf{d}}_{NP}\hat{\mathbf{E}}_{TLS} \tag{10}$$

is responsible for the dipole-dipole interaction between the QD and the NP. Taking into account that $\hat{\mathbf{E}}_{TLS} = -\hat{\mathbf{\mu}}_{TLS}r^{-3} + 3(\hat{\mathbf{\mu}}_{TLS}\cdot\mathbf{r})\mathbf{r}r^{-5}$, we obtain

$$\hat{V} = \hbar\Omega_R\left(\hat{\bar{a}}^\dagger + \hat{\bar{a}}\right)\left(\hat{\bar{\sigma}}^\dagger + \hat{\bar{\sigma}}\right), \tag{11}$$

where $\Omega_R = \left[\mathbf{\mu}_{NP}\cdot\mathbf{\mu}_{TLS} - 3\left(\mathbf{\mu}_{TLS}\cdot\mathbf{e}_r\right)\left(\mathbf{\mu}_{NP}\cdot\mathbf{e}_r\right)\right]/\hbar r_0^3$ is the Rabi frequency, r_0 is the distance between the QD and the NP, and $\mathbf{e}_r = \mathbf{r}/r$ is the unitary vector. The last term in the Hamiltonian (9) is responsible for relaxation and pumping processes.

Assuming that ω_{TLS} is close ω_{SP} we look for the solutions in the form $\hat{\bar{a}}(t) = \hat{a}(t)\exp(-i\omega_a t)$ and $\hat{\bar{\sigma}}(t) = \hat{\sigma}(t)\exp(-i\omega_a t)$, where $\hat{a}(t)$ and $\hat{\sigma}(t)$ are operators slow varying in time and ω_a is the autonomous frequency of the spaser which we seek. This is the approximation of the rotating wave[20]. Disregarding fast-oscillating terms proportional to $\exp(\pm 2i\omega_a t)$, the interaction operator $\hat{V}$ may be written the form of the Jaynes–Cummings Hamiltonian[18]

$$\hat{V} = \hbar\Omega_R(\hat{a}^\dagger\hat{\sigma} + \hat{\sigma}^\dagger\hat{a}). \tag{12}$$

Using Eqs. (3), (8), (9), and (12) and the commutation relations for operators $\hat{a}(t)$ and $\hat{\sigma}(t)$ we obtain the Heisenberg equations of motion for the operators $\hat{a}(t)$, $\hat{\sigma}(t)$, and $\hat{D}(t)$

$$\dot{\hat{D}} = 2i\Omega_R(\hat{a}^\dagger\hat{\sigma} - \hat{\sigma}^\dagger\hat{a}) - \left(\hat{D} - \hat{D}_0\right)\tau_D^{-1}, \tag{13}$$

$$\dot{\hat{\sigma}} = \left(i\delta - \tau_\sigma^{-1}\right)\hat{\sigma} + i\Omega_R\hat{a}\hat{D}, \tag{14}$$

$$\dot{\hat{a}} = \left(i\Delta - \tau_a^{-1}\right)\hat{a} - i\Omega_R\hat{\sigma}, \tag{15}$$

where $\delta = \omega_a - \omega_{TLS}$ and $\Delta = \omega_a - \omega_{SP}$ are frequency detunings. In Eqs. (13)-(15), to take into account relaxation processes (the Γ-term in Eq. (9)), we phenomenologically added terms proportional to $\tau_a^{-1}, \tau_\sigma^{-1}$, and τ_D^{-1}, which account for the relaxation processes for the SP annihilation operator, the QD polarization, and the occupancy operators, respectively[18]. The term D_0 describes pumping[21,22] and corresponds to the population inversion in the absence of the NP. Due to strong dissipation, the described scheme of quantization is approximate; at the same time, this allows us to neglect quantum fluctuations and correlations and consider $\hat{D}(t)$, $\hat{\sigma}(t)$, and $\hat{a}(t)$ as c-numbers. In this case, the Hermitian conjugation turns into the complex conjugation[23-26]. Note that the quantity $D(t)$ that describes the difference in populations of excited and ground states of the QD is a real quantity because the corresponding operator is Hermitian. The quantities $\sigma(t)$ and $a(t)$ are the complex amplitudes of the dipole oscillations of the QD and SP, respectively.

The system of Eqs. (13)-(15) has stationary solutions, which depend on the pumping level D_0. For D_0 smaller than the threshold value

$$D_{th} = \frac{1 + \left[\left(\omega_{SP} - \omega_{TLS}\right)\tau_a\tau_\sigma / \left(\tau_a + \tau_\sigma\right)\right]^2}{\Omega_R^2\tau_a\tau_\sigma}, \tag{16}$$

there is only the trivial solution $a = \sigma = 0$, $D = D_0$. For $D_0 > D_{th}$ the second stationary solution arises:

$$a = \frac{e^{i\varphi}}{2}\sqrt{\frac{(D_0 - D_{th})\tau_a}{\tau_D}}, \quad \sigma = \frac{e^{i\psi}}{2}\sqrt{\frac{(D_0 - D_{th})(\Delta^2 + \tau_a^{-2})\tau_a}{\Omega_R^2\tau_D}}, \quad \cos\left(\psi - \varphi\right) = \tau_a\Delta\left(1 + \Delta^2\tau_a^2\right)^{-1/2}. \tag{17}$$

In this case, the trivial solution corresponding to the absence of SPs is unstable, while the stable solution corresponds to laser generation of SPs (spasing) with the frequency[19]

$$\omega_a = \left(\omega_{SP}\tau_a + \omega_{TLS}\tau_\sigma\right)\big/\left(\tau_a + \tau_\sigma\right). \tag{18}$$

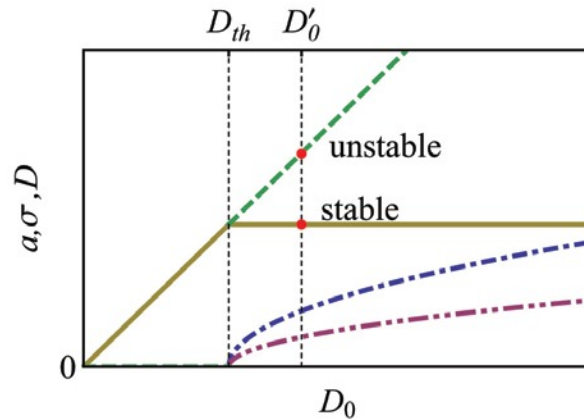The stationary values of a, σ, and D are shown in Figure 1.

Figure 1. (Color online) Stationary amplitudes a and σ are shown by dash-double dotted and dash-dotted lines, respectively. The stable solution for D is shown by the solid line. The unstable solution appearing for $D > D_{th}$ is shown by the dashed line. For $D = D_0'$ (also shown in Figure 2) the stable and unstable solutions of D are marked by red dots.

3. SPASER IN THE EXTERNAL ELECTROMAGNETIC FIELD

The Hamiltonian of a spaser driven by an external field of optical wave, which is assumed to be a classical field, $E_{OW}(t) = E\cos\nu t$, can be written in the form (see Refs. 26-28 for details)

$$\hat{H}_{eff} = \hat{H} + \hbar\Omega_1\left(\hat{\tilde{a}}^\dagger + \hat{\tilde{a}}\right)\left(e^{i\nu t} + e^{-i\nu t}\right) + \hbar\Omega_2\left(\hat{\tilde{\sigma}}^\dagger + \hat{\tilde{\sigma}}\right)\left(e^{i\nu t} + e^{-i\nu t}\right), \tag{19}$$

where $\hat{H}$ is given by Eqs. (3), (8), (9), and (12), $\Omega_1 = -\mu_{NP}E/\hbar$, and $\Omega_2 = -\mu_{TLS}E/\hbar$. As before, using the approximation of the rotating wave for slow varying amplitudes, $\hat{\tilde{a}}(t) \equiv \hat{a}(t)\exp(-i\nu t)$ and $\hat{\tilde{\sigma}}(t) \equiv \hat{\sigma}(t)\exp(-i\nu t)$, we obtain equations of motion for the operators $\hat{a}$, $\hat{\sigma}$, and $\hat{D}$:

$$\dot{\hat{D}} = 2i\Omega_R(\hat{a}^\dagger\hat{\sigma} - \hat{\sigma}^\dagger\hat{a}) + 2i\Omega_2(\hat{\sigma} - \hat{\sigma}^\dagger) - \tau_D^{-1}\left(\hat{D} - \hat{D}_0\right), \tag{20}$$

$$\dot{\hat{\sigma}} = (i\delta_E - \tau_\sigma^{-1})\hat{\sigma} + i\Omega_R\hat{a}\hat{D} + i\Omega_2\hat{D}, \tag{21}$$

$$\dot{\hat{a}} = (i\Delta_E - \tau_a^{-1})\hat{a} - i\Omega_R\hat{\sigma} - i\Omega_1, \tag{22}$$

where $\Delta_E = \nu - \omega_{SP}$ and $\delta_E = \nu - \omega_{TLS}$ are frequency detunings in the external optical field. In the next section, using Eqs. (20)-(22) we demonstrate that spasers above the pumping threshold can be used for Joule loss compensation.

Note that in the absence of the QD, the polarizability of the NP corresponding to the stationary solution of the system of Eqs. (20)-(22), $\dot{\hat{a}} = \dot{\hat{\sigma}} = 0$, has the form

$$\alpha r_{NP}^{-3} = \frac{-3}{\Delta_{SP} + i\tau_a^{-1}}\left(\frac{\partial\varepsilon_{NP}(\omega)}{\partial\omega}\right)^{-1}, \tag{23}$$

Generally, $\varepsilon_{NP}(\omega)$ is an effective permittivity of the NP in the matrix. However, for large enough NPs it can be considered as the bulk permittivity of the NP's metal. In the slowly varying amplitude approximation, i.e. for a small detuning $\Delta_{SP} \ll 1$, Eq. (23) reduces to the classical expression for the polarizability

$$\alpha^{class} r_{NP}^{-3} = \frac{\varepsilon_{NP}(\omega) - \varepsilon_M}{\varepsilon_{NP}(\omega) + 2\varepsilon_M}. \tag{24}$$

We look for a stationary solution of the system of equations (20)-(22). The stationary values of D satisfy a cubic equation and are shown in Figure 2 as a function of the amplitude of the external field E. In Figure 2a, for $\Delta = 0$, $E = 0$ and $D_0 \geq D_{th}$, two points, stable and unstable, correspond to the points marked by dots in Figure 1.

Only the lower branch of the synchronization region corresponds to the stable solution. The stationary solutions at zero external field and with no detuning ($\Delta_E = 0$) are shown in Figure 1. When detuning is present, the stable stationary solution exists for $E > E_{Synch}(\Delta_E)$ only (Figure 2b). Thus, $E_{Synch}(\Delta_E)$ is a lower boundary of the region in which the spaser is synchronized by an external wave. Such threshold behavior is characteristic for self-oscillating systems in the presence of the external periodic driving force[29]. The region in which the synchronization takes place is known as the Arnold tongue. This result is confirmed by our numerical simulation shown in Figure 3.
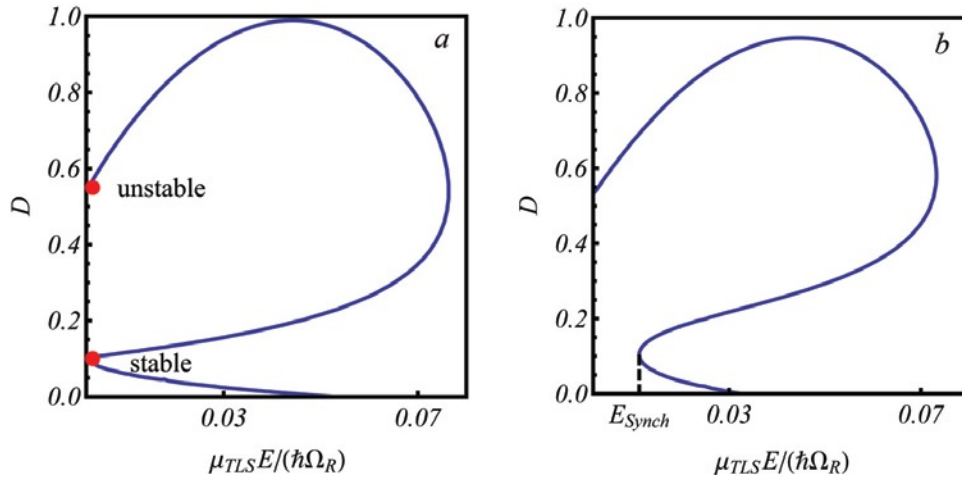
Figure 2. (Color online) The stationary values of D as a function of the amplitude of the external field for (*a*) zero ($\Delta = 0$) and (*b*) non-zero ($\Delta = 10^{11} s^{-1}$) detuning. For both graphs $\tau_a = 10^{-14} s$, $\tau_\sigma = 10^{-11} s$, $\tau_D = 0.5 \cdot 10^{-14} s$, $\Omega_R = 10^{13} s^{-1}$, and $D_0 = D_0' = 0.55$.
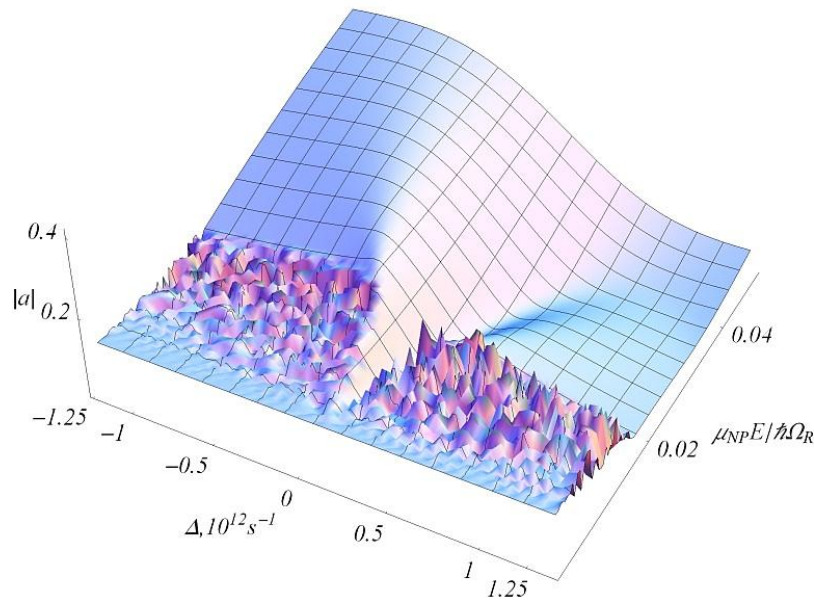

Figure 3. (Color online) The dependence of the plasmon dipole moment on the amplitude of the external field and the frequency detuning Δ. The speckle structure at low values of E corresponds to the chaotic behavior of the dipole moment.

To obtain an analytical estimate of the Arnold tongue boundary, we find the solution of Eqs. (20)–(22) in the first approximation with respect to the field. Using the substitution $a = |a|\exp(i\varphi)$ and $\sigma = |\sigma|\exp(i\psi)$ in Eq. (15), we obtain

$$|\dot{a}|\exp(i\varphi) + i\dot{\varphi}|a|\exp(i\varphi) = \left(i\Delta_E - \tau_a^{-1}\right)|a|\exp(i\varphi) - i\Omega_R|\sigma|\exp(i\psi) - i\Omega_1. \tag{25}$$

By dividing Eq. (25) by $a = |a|\exp(i\varphi)$ its imaginary part can be reduced to

$$\dot{\varphi} = \Delta_E - \Omega_R \frac{|\sigma|}{|a|}\cos(\psi - \varphi) - \frac{\Omega_1}{|a|}\cos\varphi. \tag{26}$$

Now, using the values of $|a|, |\sigma|$ and $\cos(\psi - \varphi)$ defined by Eq. (17) we obtained an equation for a phase φ:

$$\dot{\varphi} = -\frac{\partial U(\varphi)}{\partial \varphi}. \tag{27}$$

The dynamics of the phase φ can be viewed as the motion of an overdamped particle sliding along the potential profile $U(\varphi) = -\Delta_E \varphi + \Omega_1 \sin \varphi / |a|$ in a viscous liquid (Figure 4). For a small field and/or large detuning, $|\Omega_1| < |a\Delta_E|$, the phase difference of the system and the external field increases monotonically. The velocity of the "particle" oscillates; the period of oscillations tends to infinity as the field tends to the critical value $|\Omega_1| = |a\Delta_E|$. For $|\Omega_1| > |a\Delta_E|$, the "particle" is trapped in one of the minima of the potential function. In this regime, the oscillation of the system is synchronized and the phase difference is time independent. Thus, for small fields, $E \ll \hbar\Omega_R / \mu_{NP}$, the Arnold tongue has a shape of a wedge.
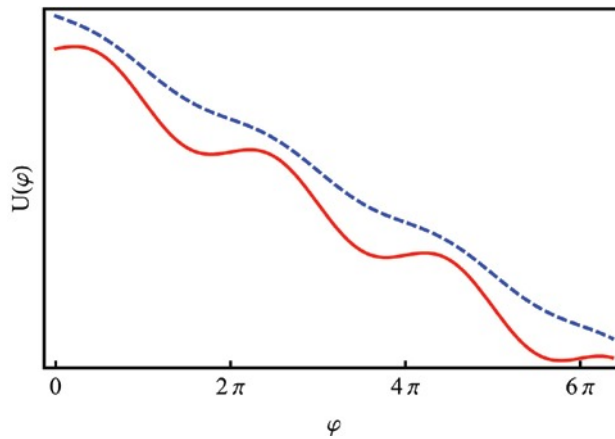

Figure 4. (Color online) The potential $U(\varphi)$ for $|\Omega_1| > |a\Delta_E|$ (dashed line) and $|\Omega_1| < |a\Delta_E|$ (solid line).

When $\Delta \to 0$ the threshold field value E_{synch} is determined by the equation $\left(\mu_{NP} E_{Synch} / \hbar\right)^2 = \left(D_0 - D_{th}\right)\Delta^2 \left(\tau_a / 4\tau_D\right)$. For large values of the detuning, E_{Synch} becomes independent of Δ_E (see Figure 3). Taking into account that for plasmonic NPs $\tau_a \sim 10^{-14} s^{-1}$ and $\tau_\sigma \sim 10^{-11} s^{-1}$, one can estimate the asymptotic value of the Arnold tongue boundary, E_{Synch}^*. Our numerical calculations show that $E_{Synch}(\Delta_E)$ tends to a plateau for $\Delta_E \sim 2 \cdot 10^{11} s^{-1}$, which gives $E_{Synch}^* \sim 3 \cdot 10^3 V/m$. The detailed investigation of the dependence of the plasmon dipole moment on the amplitude of the external field for different values of the detuning shows that there are three regimes. For $E < E_{Synch}(\Delta_E)$, the point (Δ_E, E) is outside of the Arnold tongue and the spaser is in the stochastic regime. Inside the Arnold tongue, for weak fields, the amplitude of the dipole moment of the NP depends mainly on pumping and weakly on the amplitude of the external electromagnetic field (Figure 5). Finally, the linear response regime occurs for very high values of the electric field, $E > 0.5 \times 10^6$ V/m, when the coupling of the NP with external field becomes comparable with the coupling between the NP and the QD. Moreover, our numerical calculations show that for a very strong field, the population inversion of the QD decreases, the excitation of SPs by QDs is inhibited, and the spaser becomes just a lossy NP.
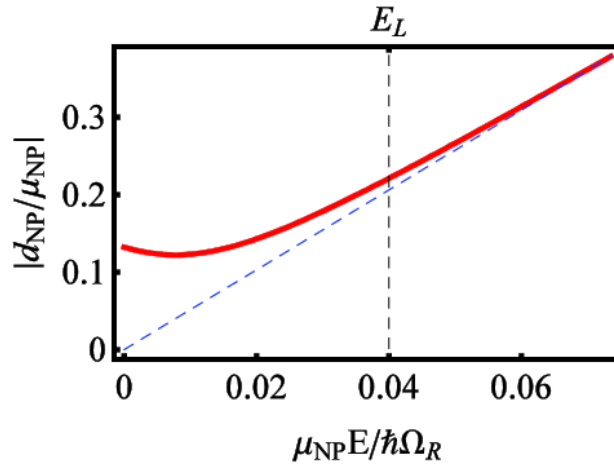
Figure 5. The dependence of the plasmon dipole moment on the amplitude of the external field for zero frequency detuning.

4. EXACT COMPENSATION OF THE EXTERNAL FIELD

Without pumping, $D_0 = -1$, the frequency dependence of the dipole moment of the NP is similar to that of a classical dipole: its real part may be positive or negative depending on the detuning, Δ_E, whereas the imaginary part is always positive due to losses. This corresponds to the energy transfer from the external field to the spaser. When the pumping is present, the imaginary part of the dipole may change sign and become negative for some values of Δ_E (see Figure 6) signifying the amplification of the incident wave.
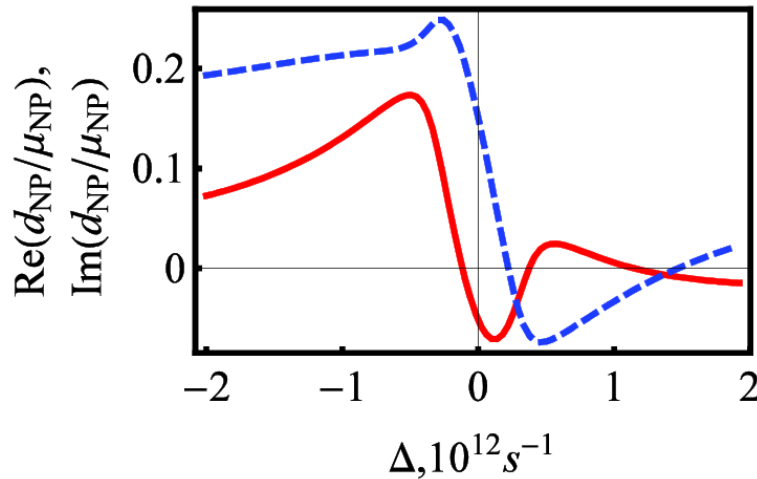

Figure 6. (Color online) The dependences of the real (solid line) and imaginary (dashed line) parts of the NP dipole moment on the frequency detuning Δ_E for a value of the amplitude of the external field greater than the synchronization threshold, $E > E_{Synch}(\Delta_E)$.

Figure 6 shows that for fixed E there are two values of Δ_E for which an exact compensation of losses can be achieved. These points form a single curve $E_{Comp}(\Delta_E)$ in the $\{E, \Delta_E\}$- plane (Figure 7). The equation of this curve is[27]

$$\left(\frac{\mu_{NP}E_{comp}(\Delta_E)}{\hbar}\right)^2 = \frac{\left\{-\left(\frac{\tau_D\tau_\sigma^3}{\tau_a}\right)\Delta_E^4 + \left[D_0\Omega_R\tau_\sigma^3\left(\frac{\mu_{TLS}}{\mu_{NP}}\right)\right]\frac{\Delta_E^3}{\tau_D} - \left[\left(\frac{\tau_\sigma}{\tau_D}\right) - \Omega_R^2 D_0\frac{\tau_a\tau_\sigma^2}{\tau_D}\right]\Delta_E^2\right\}}{4\left[\tau_\sigma\Delta_E\left(\frac{\mu_{TLS}}{\mu_{NP}}\right) + \tau_a\Omega_R\right]^2}. \tag{28}$$

As $\Delta_E \to 0$, this expression transforms into

$$\left(\frac{\mu_{NP}E_{comp}(\Delta_E)}{\hbar}\right)^2 = \frac{(D_0 - D_{th})\Delta_E^2\tau_\sigma^2}{\tau_D\tau_a}. \tag{29}$$

Thus, $E_{Comp} \propto (D_0 - D_{th})^{1/2}\Delta_E$. This curve lies inside the Arnold tongue. Having estimated $\Omega_R \sim \mu_{NP}\mu_{TLS}/(\hbar r^3) \sim 5\cdot10^{12}\,s^{-1}$ ($r \sim r_{NP}$), we obtain $D_{th} = 0.4$.

In Figure 7 the dipole phase as a function of E and Δ obtained by the numerical solution of Eqs. (20)-(22) is shown. The rupture line is the line given by Eq. (28). The phase difference on this line is equal to π, so that the exact compensation occurs. Interestingly, one can expect that within the Arnold tongue the system reaches $E_{Comp}(\Delta_E)$ automatically. If the amplitude of the travelling wave is greater than $E_{Comp}(\Delta_E)$, the energy is transferred from the wave to spasers and the amplitude of the travelling wave decreases until it reaches the value of $E_{Comp}(\Delta_E)$. If the amplitude of the travelling wave corresponds to a point below the curve of the exact compensation, then the energy is transferred from spasers to the wave and the wave amplitude increases. Thus, eventually the wave starts travelling with the amplitude independent on the external wave.
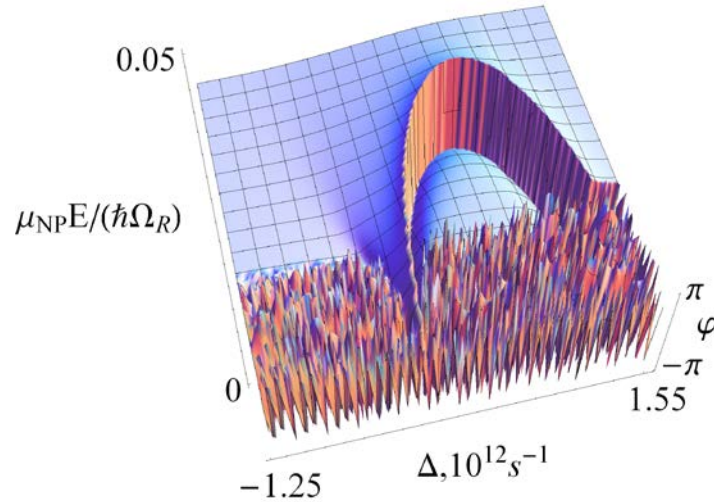

Figure 7. (Color online) The dependence of $\phi = \tan^{-1}(\mathrm{Im}\,d_{NP}/\mathrm{Re}\,d_{NP})$ on the amplitude of the external field E and the detuning Δ_E. The smooth part of the surface corresponds to the Arnold tongue where the spaser is synchronized by the external field. At the discontinuity line, on which $\phi = \pi$, the loss is exactly compensated.

The above argument is based on the analysis of a single spaser. In a system of spaser, due to spaser interactions, collective effects may arise. These effects may qualitatively change the external wave propagation in the active metamaterial. In the next section we discuss wave propagation in a regular linear chain of interacting spasers.

5. SPASER CHAIN

In this this section we consider collective excitations of spaser auto-oscillations above the generation threshold in the one-dimensional chain of spasers[30]. We show that depending on the values of the coupling constants, two different scenarios for the stationary behavior of a chain of interacting spasers may be realized: (1) all the spasers are synchronized and oscillate with a unique phase or (2) a nonlinear autowave travels along the chain[31-35]. In the latter scenario, the collective mode is a wave of dipole moment oscillations traveling along the chain (see Ref. 16 and references therein).

5.1. Synchronization of two spasers

As far back as to Huygens, it has been known that auto-oscillating systems can be synchronized by even a weak interaction[29]. Before considering collective excitations of a spaser chain, we discuss the behavior of two coupled spasers. In order to do this, we generalize the system of equations (13)-(14) by introducing coupling terms:

$$\dot{\hat{D}}_1 = 2i\Omega_{R1}(\hat{a}_1^\dagger\hat{\sigma}_1 - \hat{\sigma}_1^\dagger\hat{a}_1) + 2i\Omega_{NP-TLS}(\hat{a}_2^\dagger\hat{\sigma}_1 - \hat{\sigma}_1^\dagger\hat{a}_2) + 2i\Omega_{TLS-TLS}(\hat{\sigma}_2^\dagger\hat{\sigma}_1 - \hat{\sigma}_1^\dagger\hat{\sigma}_2) - \tau_{D1}^{-1}\left(\hat{D}_1 - \hat{D}_{01}\right), \tag{30}$$

$$\dot{\hat{D}}_2 = 2i\Omega_{R2}(\hat{a}_2^\dagger\hat{\sigma}_2 - \hat{\sigma}_2^\dagger\hat{a}_2) + 2i\Omega_{NP-TLS}(\hat{a}_1^\dagger\hat{\sigma}_2 - \hat{\sigma}_2^\dagger\hat{a}_1) + 2i\Omega_{TLS-TLS}(\hat{\sigma}_2^\dagger\hat{\sigma}_1 - \hat{\sigma}_1^\dagger\hat{\sigma}_2) - \tau_{D2}^{-1}\left(\hat{D}_2 - \hat{D}_{02}\right), \tag{31}$$

$$\dot{\hat{\sigma}}_1 = \left(i\delta - \tau_\sigma^{-1}\right)\hat{\sigma}_1 + i\Omega_{R1}\hat{a}_1\hat{D}_1 + i\Omega_{NP-TLS}\hat{a}_2\hat{D}_1 + i\Omega_{TLS-TLS}\hat{\sigma}_2\hat{D}_1, \tag{32}$$

$$\dot{\hat{\sigma}}_2 = \left(i\delta - \tau_\sigma^{-1}\right)\hat{\sigma}_2 + i\Omega_{R2}\hat{a}_2\hat{D}_2 + i\Omega_{NP-TLS}\hat{a}_1\hat{D}_2 + i\Omega_{TLS-TLS}\hat{\sigma}_1\hat{D}_2, \tag{33}$$

$$\dot{\hat{a}}_1 = \left(i\Delta - \tau_a^{-1}\right)\hat{a}_1 - i\Omega_{R1}\hat{\sigma}_1 - i\Omega_{NP-NP}\hat{a}_2 - i\Omega_{NP-TLS}\hat{\sigma}_2, \tag{34}$$

$$\dot{\hat{a}}_2 = \left(i\Delta - \tau_a^{-1}\right)\hat{a}_2 - i\Omega_{R2}\hat{\sigma}_2 - i\Omega_{NP-NP}\hat{a}_1 - i\Omega_{NP-TLS}\hat{\sigma}_1. \tag{35}$$

Indexes 1 and 2 label the quantities corresponding to the first and to second spasers, respectively,

$$\Omega_{NP-NP} = \left[\boldsymbol{\mu}_{NP1}\cdot\boldsymbol{\mu}_{NP2} - 3\left(\boldsymbol{\mu}_{NP1}\cdot\mathbf{e}_{NP-NP}\right)\left(\boldsymbol{\mu}_{NP2}\cdot\mathbf{e}_{NP-NP}\right)\right]\left(\hbar r_{NP-NP}^3\right)^{-1}$$

is a coupling constant between neighboring NP,

$$\Omega_{NP-TLS} = \left[\boldsymbol{\mu}_{NP1}\cdot\boldsymbol{\mu}_{TLS2} - 3\left(\boldsymbol{\mu}_{NP1}\cdot\mathbf{e}_{NP-TLS}\right)\left(\boldsymbol{\mu}_{TLS2}\cdot\mathbf{e}_{NP-TLS}\right)\right]\left(\hbar r_{NP-TLS}^3\right)^{-1}$$

$$= \left[\boldsymbol{\mu}_{NP2}\cdot\boldsymbol{\mu}_{TLS1} - 3\left(\boldsymbol{\mu}_{NP2}\cdot\mathbf{e}_{NP-TLS}\right)\left(\boldsymbol{\mu}_{TLS1}\cdot\mathbf{e}_{NP-TLS}\right)\right]\left(\hbar r_{NP-TLS}^3\right)^{-1}$$

is a coupling constant between neighboring QD and NP,

$$\Omega_{TLS-TLS} = \left[\boldsymbol{\mu}_{TLS1}\cdot\boldsymbol{\mu}_{TLS2} - 3\left(\boldsymbol{\mu}_{TLS1}\cdot\mathbf{e}_{TLS-TLS}\right)\left(\boldsymbol{\mu}_{TLS2}\cdot\mathbf{e}_{TLS-TLS}\right)\right]\left(\hbar r_{TLS-TLS}^3\right)^{-1}$$

is a coupling constant between neighboring QDs, $\mathbf{e}_{NP-NP}$, $\mathbf{e}_{NP-TLS}$, and $\mathbf{e}_{TLS-TLS}$ are unit vectors pointing from the NP to the neighboring NP, from the NP to the QD, and from the QD to the neighboring QD, respectively, r_{NP-NP}, r_{NP-TLS}, and $r_{TLS-TLS}$ are the corresponding distances. These coupling constants have the dimension of frequency. At optical frequencies, $\sim 5\cdot10^{15}\,s^{-1}$, for typical QD and NP supposing that $r_{NP-NP}, r_{NP-TLS}, r_{TLS-TLS} \sim 50nm$, we obtain $\Omega_{NP-NP} \sim 10^{13}\,s^{-1}$, $\Omega_{NP-TLS} \sim 10^{12}\,s^{-1}$, and $\Omega_{TLS-TLS} \sim 10^{11}\,s^{-1}$.

The values of the coupling constants depend on the orientation of corresponding dipoles. In particular, if the dipoles are parallel, then $\Omega_{1-2} = \gamma_i\left(\boldsymbol{\mu}_1\cdot\boldsymbol{\mu}_2\right)/\left(\hbar r_{12}^3\right)$ with $\gamma_1 = -2$ for the longitudinal and $\gamma_{2,3} = 1$ for transverse modes. Below we imply that the γ factor is included in the definition of the coupling constants.

One can show that for $D_0 < D_{th}$, where

$$D_{th} = \frac{1 + \left(\Omega_{NP-NP}^{eff}\tau_\sigma\right)^2}{\left(\Omega_R + 2\Omega_{NP-TLS}\right)^2 \tau_a \tau_\sigma}, \tag{36}$$

only the trivial solution, $a_{1,2} = 0$, $\sigma_{1,2} = 0$ and $D_{1,2} = D_{01,2}$, satisfies the system of equations (30)-(35). In Eq. (36) we introduce the notation $\Omega_{NP-NP}^{eff} = 2\Omega_{NP-NP}\tau_a / (\tau_a + \tau_\sigma)$. For $D_0 > D_{th}$, by the direct substitution one can verify that if $\Omega_{NP-TLS} > 0$, then

$$\hat{a}_1 = \hat{a}_2, \quad \hat{\sigma}_1 = \hat{\sigma}_2, \hat{D}_1 = \hat{D}_2, \tag{37}$$

is the stationary solution to Eqs. (30)-(35). For $\Omega_{NP-TLS} < 0$ the stationary solution is

$$\hat{a}_1 = -\hat{a}_2, \quad \hat{\sigma}_1 = -\hat{\sigma}_2, \hat{D}_1 = \hat{D}_2. \tag{38}$$

Thus, when the pumping exceeds the threshold value (36), a couple of identical spasers behave like a single spaser for which the spasing occurs at the frequency

$$\omega = \Omega_{NP-NP}^{eff} + \frac{\omega_{SP}\tau_a + \omega_{TLS}\tau_\sigma}{\tau_a + \tau_\sigma}. \tag{39}$$

In this case, the phase locking occurs, so that the phase difference $\Delta\varphi$ between the oscillations is equal to zero and π, if $\Omega_{NP-TLS} > 0$ and $\Omega_{NP-TLS} < 0$, respectively. This result is confirmed by computer simulation in time domain that shows that the system arrives at the stationary state given by Eqs. (36)-(39) independent of initial conditions.

5.2. Excitations in a chain of spasers

In this section we discuss a chain of spasers schematically shown in Figure 8. In order to describe this system we have to include spaser-spaser interacting terms into Hamiltonian (9):

$$\hat{H} = \sum_n \left[\hbar\omega_{SP}\hat{a}_n^+\hat{a}_n + \hbar\omega_{TLS}\hat{\sigma}_n^+\hat{\sigma}_n + \hbar\Omega_R(\hat{a}_n^+\hat{\sigma}_n + \hat{a}_n\hat{\sigma}_n^+) + \frac{1}{2}\hbar\Omega_{NP-NP}(\hat{a}_n^+\hat{a}_{n-1} + \hat{a}_n\hat{a}_{n-1}^+ + \hat{a}_n^+\hat{a}_{n+1} + \hat{a}_n\hat{a}_{n+1}^+) \right.$$
$$\left. + \frac{1}{2}\hbar\Omega_{NP-TLS}(\hat{\sigma}_n^+\hat{a}_{n-1} + \hat{\sigma}_n\hat{a}_{n-1}^+ + \hat{\sigma}_n^+\hat{a}_{n+1} + \hat{\sigma}_n\hat{a}_{n+1}^+) + \frac{1}{2}\hbar\Omega_{TLS-TLS}(\hat{\sigma}_n^+\hat{\sigma}_{n-1} + \hat{\sigma}_n\hat{\sigma}_{n-1}^+ + \hat{\sigma}_n^+\hat{\sigma}_{n+1} + \hat{\sigma}_n\hat{\sigma}_{n+1}^+) \right], \tag{40}$$

where the summation is performed over the spasers. The meaning of the interaction constants Ω_{NP-NP}, Ω_{NP-TLS}, and $\Omega_{TLS-TLS}$ is clear from Figure 8.
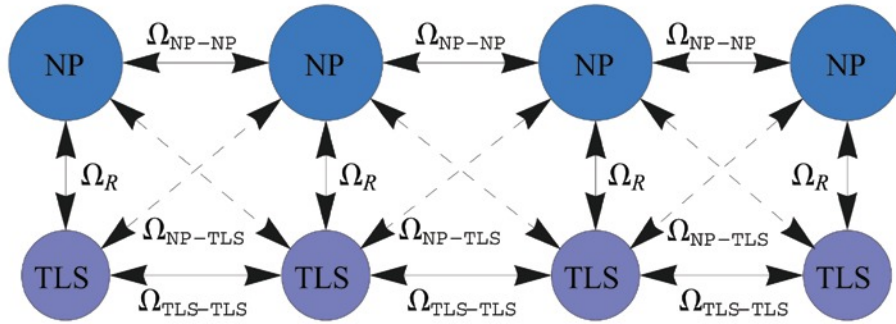

Figure 8. (Color online) Schematic of the chain of spasers.

Following the procedure described in Section 2, we arrive at the equations of motion of the spasers:

$$\dot{\hat{D}}_n = 2i\left(\Omega_R + 2\Omega_{NP-TLS}\cos kb\right)\left(\hat{a}_n^+\hat{\sigma}_n - \hat{a}_n\hat{\sigma}_n^+\right) - \left(\hat{D}_n - \hat{D}_{0n}\right)\tau_D^{-1}, \tag{41}$$

$$\dot{\hat{\sigma}}_n = (i\delta - \tau_\sigma^{-1})\hat{\sigma}_n + i(\Omega_R + 2\Omega_{NP-TLS}\cos kb)\hat{a}_n\hat{D}_n + 2i\Omega_{TLS-TLS}\hat{\sigma}_n\hat{D}_n\cos kb, \tag{42}$$

$$\dot{\hat{a}}_n = -\left[\left(1 + i\Omega_{NP-NP}^{eff}\tau_\sigma\cos kb\right)\tau_a^{-1}\right]\hat{a}_n - i(\Omega_R + 2\Omega_{NP-TLS}\cos kb)\hat{\sigma}_n, \tag{43}$$

where b is a distance between neghbouring spasers. To beging with, we take into account interactions between NPs only, assuming that $\Omega_{NP-TLS} = \Omega_{TLS-TLS} = 0$. In this case, one can show that when the pumping exceeds the threshold value

$$D_{th}(k) = \left[1 + \left(\Omega_{NP-NP}^{eff}\,\tau_\sigma\right)^2\cos^2 kb\right]\Big/\left(\Omega_R^2\tau_a\tau_\sigma\right), \tag{44}$$

the stationary solution of Eqs. (41)-(43) is a harmonic wave, $a_{n+1,k} = a_{n,k}\exp(ikb)$, which dispersion equation has the form

$$\omega_k = \omega_a + \Omega_{NP-NP}^{eff}\cos kb. \tag{45}$$

where the generation frequency of a single spaser, ω_a, is given by Eq. (18).

Thus, even though the chain of spasers is a non-linear system, *harmonic* waves can travel in it. The dispersion equation for these waves is similar to the dispersion equation for the wave of dipole moments traveling along the linear system of lossless chain of spherical particles in the absence of QDs[16,36,37]. Indeed, in the latter case, the dispersion equation for one longitudinal and two transverse modes has the form

$$\omega(k) = \omega_{SP} + \left(\gamma_i\omega_1^2/\omega_{SP}\right)\cos kb, \tag{46}$$

where $\gamma_1 = -2$ for longitudinal and $\gamma_{2,3} = 1$ for transverse modes. In Ref. 38 it has been shown that $\omega_1^2 = r_{NP}^3\omega_{pl}^2/3b^3$, where ω_{pl} is the plasmon frequency in the Drude type of dispersion, $\varepsilon_{NP} = 1 - \omega_{pl}^2/\omega^2$. Taking into account that $|\boldsymbol{\mu}_{NP}| = \sqrt{3\hbar r_{NP}^3/(\partial\operatorname{Re}\varepsilon_{NP}/\partial\omega)}$ and the assumption[39] that the surface plasmon resonance occurs at $\omega_{SP} = \omega_{pl}/\sqrt{3}$, the factor in Eq. (46) can be recast as

$$\Omega_{NP-NP}^{eff} = 2\Omega_{NP-NP}\frac{\tau_a}{\tau_a + \tau_\sigma} = \frac{2\tau_a}{\tau_a + \tau_\sigma}\gamma_i\frac{\boldsymbol{\mu}_{NP}^2}{\hbar b^3} = \frac{\tau_a}{\tau_a + \tau_\sigma}\gamma_i\frac{\omega_1^2}{\omega_{SP}},$$

which up to the factor $\tau_a/(\tau_a + \tau_\sigma)$ coincides with the factor in Eq. (45). In the case of absence of the QD, we can put $\tau_\sigma = 0$ and arrive at exact match.

It should be noted that Eqs. (45) and (46) are valid for $k > k_0$ only. For $k < k_0$ the waves become leaky. Indeed, as we mentioned in Introduction, the radiation is suppressed for $(k_0 r_{NT-TLS})^{-3} \ll 1$. However, when k is smaller than k_0, k^{-1} becomes the new length scale of the system so that the efficiency of the radiative emission, $(k_0/k)^{-3} \geq 1$, becomes substantial suppressing the SP amplification.

Thus, we obtain that the dispersion equations for the harmonic waves traveling along a chain of plasmonic NPs and a chain of nonlinear spasers are nearly the same. However, there is a principal difference between the waves in these systems. In the linear system, the wave amplitude can take an arbitrary value, while in the nonlinear case the amplitude is determined by the pumping:

$$a_{n,k} = \frac{1}{2}\exp(i\varphi)\sqrt{\left[D_0 - \left(1 + \left(\Omega_{NP-NP}^{eff}\tau_\sigma\right)^2\cos^2 kb\right)\Big/\Omega_R^2\tau_a\tau_\sigma\right]\frac{\tau_a}{\tau_\sigma}}. \tag{47}$$

In addition, while for waves in a linear system of NPs, the superposition principle is applied, it does not work for the spaser chain. The wave stability analysis shows that only the autowaves with $k = \pm\pi/2b$ are stable. All other autowaves are unstable, so that any initial perturbation evolves into one of two stable waves. Also, in contrast to a typical nonlinear wave which has a form of a soliton or a kink[40], the obtained wave is perfectly harmonic.

In the linear case of a NP chain, if we express the initial condition as a sum of harmonic waves, each harmonics has a fixed value of the Poynting vector. Then, each harmonics generates two waves with the same $\omega(k)$ travelling in opposite directions and having the sum of Poynting vectors equal to the initial one. Ultimately, a number of harmonic waves can travel simultaneously. The total number is determined by the initial conditions. In our nonlinear case of a spaser chain, any initial condition evolves into a single wave which direction of propagation depends on the initial conditions. It is the total Poynting vector of the initial state that determines the direction of propagation of a single surviving wave. Note, that in the case of $\Omega_{NP-TLS} = \Omega_{TLS-TLS} = 0$, there are no stable solutions with $kb = 0$ and $kb = \pm\pi$. Thus, in a chain in which spasers are coupled via interaction of NPs only, the synchronous oscillations of spasers do not occur.

Turning on the coupling between a NP and a QD of the neighboring spasers, Ω_{NP-TLS}, qualitatively changes the dynamics of the system. First, the threshold value of pumping becomes

$$D_{th}(k) = \frac{1 + \left(\tau_\sigma \Omega_{NP-NP}^{eff}\right)^2 \cos^2 kb}{(\Omega_R + 2\Omega_{NP-TLS} \cos kb)^2 \tau_a \tau_\sigma}. \tag{48}$$

For $\Omega_R > 0$, an increase of $\Omega_{NP-TLS} > 0$, results in a decrease of the wavenumber of the stable solution, which reaches zero at some value of Ω_{NP-TLS}^* (see Figure 9). Thus, Ω_{NP-TLS}^* divides dispersive waves and waves with $k = \pm\pi / b$ or $k = 0$. Beyond this point, for any the wave number remains zero when Ω_{NP-TLS} increases. The stability condition of the solutions of the equations of motions coincides with the minimum of $D_{th}(k)$.

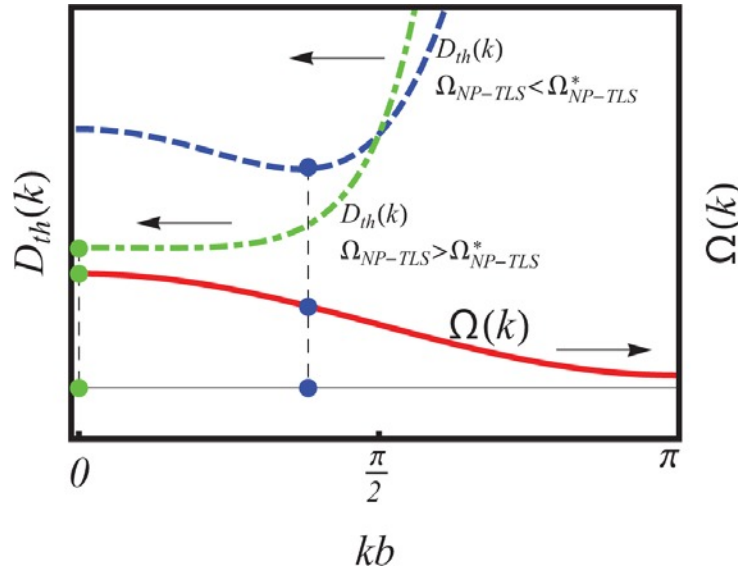Figure 9. (Color online) The dependence of the threshold pumping on the wavenumber k for $\Omega_{NP-TLS} < \Omega_{NP-TLS}^*$ (dashed curve) and $\Omega_{NP-TLS} > \Omega_{NP-TLS}^*$ (dot-dashed curve). The solid curve shows the dependence $\omega(k)$.

The values of k corresponding to min/max values of Eq. (48) are determined by equations

$$\sin kb = 0, \tag{49}$$

$$\cos kb = 2\Omega_{NP-TLS} / \left(\tau_\sigma \Omega_{NP-NP}^{eff}\right)^2 \Omega_R. \tag{50}$$

When $2\Omega_{NP-TLS}\left(\tau_\sigma\Omega_{NP-NP}^{eff}\right)^{-2}\leq\Omega_R$, solutions of Eqs. (49) and (50) correspond to maximum and minimum values of $D_{th}(k)$, respectively. If $2\Omega_{NP-TLS}\left(\tau_\sigma\Omega_{NP-NP}^{eff}\right)^{-2}>\Omega_R$, the minimum of $D_{th}(k)$ is achieved for wavenumbers given by the solutions of Eq. (50). This gives the value of Ω_{NP-TLS}^*:

$$\Omega_{NP-TLS}^*=\frac{1}{2}\left(\tau_\sigma\Omega_{NP-NP}^{eff}\right)^2\Omega_R. \tag{51}$$

The analysis for negative values of Ω_{NP-TLS} and/or Ω_R is similar. To summarize, in the case of $\Omega_R>0$, the dependence of the wavenumber of the stable solution on the coupling constant Ω_{NP-TLS} is

$$kb=\begin{cases}\pi, & \Omega_{NP-TLS}<-\Omega_{NP-TLS}^* \\ \cos^{-1}\left(\dfrac{2\Omega_{NP-TLS}}{\left(\tau_\sigma\Omega_{NP-NP}^{eff}\right)^2\Omega_R}\right), & -\Omega_{NP-TLS}^*\leq\Omega_{NP-TLS}\leq\Omega_{NP-TLS}^* \\ 0, & \Omega_{NP-TLS}>\Omega_{NP-TLS}^*.\end{cases} \tag{52}$$

Similarly, for $\Omega_R<0$ we have

$$kb=\begin{cases}0, & \Omega_{NP-TLS}<-\Omega_{NP-TLS}^* \\ \pi-\cos^{-1}\left(\dfrac{2\Omega_{NP-TLS}}{\left(\tau_\sigma\Omega_{NP-NP}^{eff}\right)^2\Omega_R}\right), & -\Omega_{NP-TLS}^*\leq\Omega_{NP-TLS}\leq\Omega_{NP-TLS}^* \\ \pi, & \Omega_{NP-TLS}>\Omega_{NP-TLS}^*.\end{cases} \tag{53}$$

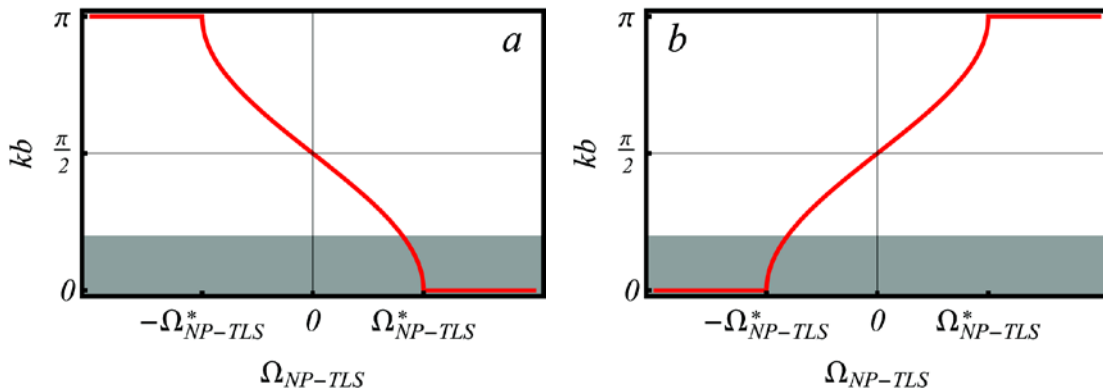The dependencies given by Eqs. (52) and (53) are shown in Figure 10.

Figure 10. (Color online) The dependencies of the stable solution of Eqs. (50)-(52) for (a) $\Omega_R>0$ and (b) $\Omega_R<0$, respectively. The shaded areas correspond to leaky wave solutions.

"Turning on" the coupling between neighboring QDs, $\Omega_{TLS-TLS}$, does not qualitatively change the dynamics of the chain. The QD-QD coupling constant is much smaller than all other coupling constants because the respective dipole moments are smaller. Retaining the lowest order terms with respect to $\Omega_{TLS-TLS}$, we obtain the dispersion equation for the traveling harmonic wave

$$\omega(k)=\omega_a+\Omega_{NP-NP}^{eff}\cos kb+\frac{2\Omega_{TLS-TLS}\tau_a}{(\tau_a+\tau_\sigma)(\Omega_R+2\Omega_{NP-TLS}\cos kb)^2}\left[\left(\omega_a-\omega_{SP}-\Omega_{NP-NP}^{eff}\tau_\sigma\tau_a^{-1}\cos kb\right)^2+\tau_a^{-2}\right]. \tag{54}$$

The wavenumbers of the stable in-phase oscillations are still either $kb = 0$ or $kb = \pi$ depending upon the sign of Ω_R. Of course, the threshold value of Ω^*_{NP-TLS} is different than the one given by Eq. (60).

Depending on the strength of the interaction between a QD and the nearest NP, either a synchronized oscillation of all the spasers or a harmonic autowave travelling along the chain may arise. Thus, the pumped QD may either excite its own spasers so that all spasers are synchronized or cooperating with the other QDs, the pumped QD may excite a plasmonic wave traveling along the chain. This is the wave of the NP polarization whose dispersion is similar to that predicted in Refs. 16,39 for linear systems. Unlike the general case of a wave propagating in a nonlinear lattice,[40] the nonlinear character of the spasers' response to an external field results neither in soliton nor in kink solutions. Rather, the response is a perfectly harmonic wave. However, unlike harmonic waves in linear systems, in a chain of spasers, (*i*) the wave has a fixed value of the wavenumber, which is determined by the minimum value of the pumping threshold and the values of the coupling constants, (*ii*) its amplitude also has a fixed value, which is determined by the pumping strength, and (*iii*) its propagation direction is determined by the initial conditions.

6. SUMMARY

Spasers are devices with a great potential for the light manipulating in the regions of the scale of tens nanometers which are much smaller than the optical wavelength. Not only can they be used as superfast devices[17], but also as active inclusions into metamaterials. The composite material based on spasers is a new nonlinear object for research with unique features. During the period in which stationary spaser oscillations are established, a spaser undergoes Rabi oscillations[28]. Therefore, its properties can be controlled by intensity of the external optical field. In the stationary regime, spasers are sensitive to the frequency and the amplitude of the external electromagnetic wave. Varying this parameters one can switch the spasing regime from stochastic oscillations to propagation of plasmon autowaves. The amplitude of these autowaves weakly depends on the amplitude of the incoming signal. It is mainly controlled by the level of pumping. Thanks to the wealth of unusual spaser properties, spaser based materials may find various applications in optoelectronics.

REFERENCES

[1]   Cai, W. and Shalaev, V., [Optical Metamaterials: Fundamentals and Applications], Springer, Dordrecht (2010).
[2]   Marques, R., Martin, F. and Sorolla, M., [Metamaterials with negative parameters: theory, design and microwave applications], Wiley (2008).
[3]   Pendry, J. B., "Negative Refraction Makes a Perfect Lens," Phys. Rev. Lett. 85(18), 3966-3969 (2000).
[4]   Kolokolov, A. A. and Skrotskii, G. V., "Interference of reactive components of an electromagnetic field," Sov. Phys. Usp. 35(12), 1089 (1992).
[5]   Vinogradov, A. P. and Dorofeenko, A. V., "Destruction of the image of the Pendry lens during detection," Opt. Commun. 25, 333-336 (2005).
[6]   Lagarkov, A. N., Sarychev, A. K., Kissel, V. N. and Tartakovsky, G., "Superresolution and enhancement in metamaterials," Phys. Usp. 52(9), 959–967 (2009).
[7]   Noginov, M. A., Podolskiy, V. A., Zhu, G., Mayy, M., Bahoura, M., Adegoke, J. A., Ritzo, B. A. and Reynolds, K., "Compensation of loss in propagating surface plasmon polariton by gain in adjacent dielectric medium," Opt. Express 16(2), 1385-1392 (2008).
[8]   Noginov, M. A., Zhu, G., Bahoura, M., Adegoke, J., Small, C., Ritzo, B. A., Drachev, V. P. and Shalaev, V. M., "The effect of gain and absorption on surface plasmons in metal nanoparticles," Appl. Phys. B 86(3), 455-460 (2006).
[9]   Popov, A. K. and Shalaev, V. M., "Compensating losses in negative-index metamaterials by optical parametric amplification," Opt. Lett. 31(14), 2169-2171 (2006).
[10]   Ramakrishna, S. A. and Pendry, J. B., "Removal of absorption and increase in resolution in a near-field lens via optical gain," Phys. Rev. B 67(20), 201101 (2003).
[11]   Sarychev, A. K. and Tartakovsky, G., "Magnetic plasmonic metamaterials in actively pumped host medium and plasmonic nanolaser," Phys. Rev. B 75(8), 085436 (2007).
[12]   Bergman, D. J. and Stockman, M. I., "Surface Plasmon Amplification by Stimulated Emission of Radiation: Quantum Generation of Coherent Surface Plasmons in Nanosystems," Phys. Rev. Lett. 90(2), 027402 (2003).

[13] Noginov, M. A., Zhu, G., Belgrave, A. M., Bakker, R., Shalaev, V. M., Narimanov, E. E., Stout, S., Herz, E., Suteewong, T. and Wiesner, U., "Demonstration of a spaser-based nanolaser," Nature 460(7259), 1110-1112 (2009).

[14] Stockman, M. I., "Spasers explained," Nat. Photon. 2(6), 327-329 (2008).

[15] Gabitov, I. R., Kennedy, B. and Maimistov, A. I., "Coherent Amplification of Optical Pulses in Metamaterials," IEEE J. Sel. Top. Quantum Electron. 16(2), 401-409 (2010).

[16] Klimov, V. V., [Nanoplasmonics], Pan Stanford Publishing, Singapore (2011).

[17] Stockman, M. I., "The spaser as a nanoscale quantum generator and ultrafast amplifier " J. Opt. 12, 024004 (2010).

[18] Scully, M. O. and Zubairy, M. S., [Quantum Optics], Cambridge University Press, Cambridge (1997).

[19] Protsenko, I. E., Uskov, A. V., Zaimidoroga, O. A., Samoilov, V. N. and O'Reilly, E. P., "Dipole nanolaser," Phys. Rev. A 71(6), 063812 (2005).

[20] Pantell, R. H. and Puthoff, H. E., [Fundamentals of quantum electronics], Wiley, New York (1969).

[21] Leonhardt, U., "Notes on waves with negative phase velocity," IEEE J. Sel. Top. Quantum Electron. 9(1), 102-105 (2003).

[22] Cummer, S. A., Popa, B.-I., Schurig, D., Smith, D. R. and Pendry, J., "Full-wave simulations of electromagnetic cloaking structures," Phys. Rev. E 74(3), 036621 (2006).

[23] Belov, P. A., Simovski, C. R. and Ikonen, P., "Canalization of subwavelength images by electromagnetic crystals," Phys. Rev. B 71(19), 193105 (2005).

[24] Pendry, J. B., Schurig, D. and Smith, D. R., "Controlling Electromagnetic Fields," Science 312(5781), 1780-1782 (2006).

[25] Liu, Z., Lee, H., Xiong, Y., Sun, C. and Zhang, X., "Far-Field Optical Hyperlens Magnifying Sub-Diffraction-Limited Objects," Science 315(5819), 1686 (2007).

[26] Andrianov, E. S., Pukhov, A. A., Dorofeenko, A. V., Vinogradov, A. P. and Lisyansky, A. A., "Forced synchronization of spaser by an external optical wave," Opt. Express 19(25), 24849-24857 (2011).

[27] Andrianov, E. S., Pukhov, A. A., Dorofeenko, A. V., Vinogradov, A. P. and Lisyansky, A. A., "Dipole Response of Spaser on an External Optical Wave," Opt. Lett. 36(21), 4302-4304 (2011).

[28] Andrianov, E. S., Pukhov, A. A., Dorofeenko, A. V., Vinogradov, A. P. and Lisyansky, A. A., "Rabi oscillations in spasers during non-radiative plasmon excitation," Phys. Rev. B 85(3), 035405 (2012).

[29] Pikovsky, A., Rosenblum, M. and Kurths, J., [Synchronization. A universal concept in nonlinear sciences], Cambridge University Press, Cambridge, (2001).

[30] Andrianov, E. S., Pukhov, A. A., Dorofeenko, A. V., Vinogradov, A. P. and Lisyansky, A. A., "Stationary behavior of a chain of interacting spasers," Phys. Rev. B 85(16), 165419 (2012).

[31] Chang, D. E., Sorensen, A. S., Hemmer, P. R. and Lukin, M. D., "Quantum Optics with Surface Plasmons," Phys. Rev. Lett. 97(5), 053002 (2006).

[32] Hill, M. T., Marell, M., Leong, E. S. P., Smalbrugge, B., Zhu, Y., Sun, M., van Veldhoven, P. J., Geluk, E. J., Karouta, F., Oei, Y.-S., Nötzel, R., Ning, C.-Z. and Smit, M. K., "Lasing in metal-insulator-metal sub-wavelength plasmonic waveguides," Opt. Express 17(13), 11107-11112 (2009).

[33] Lisyansky, A. A., Nechepurenko, I. A., Dorofeenko, A. V., Vinogradov, A. P. and Pukhov, A. A., "Channel spaser: Coherent excitation of one-dimensional plasmons from quantum dots located along a linear channel," Phys. Rev. B 84(15), 153409 (2011).

[34] Fedyanin, D. Y. and Arsenin, A. V., "Surface plasmon polariton amplification in metal-semiconductor structures," Opt. Express 19(13), 12524-12531 (2011).

[35] Flynn, R. A., Kim, C. S., Vurgaftman, I., Kim, M., Meyer, J. R., Mäkinen, A. J., Bussmann, K., Cheng, L., Choa, F.-S. and Long, J. P., "A room-temperature semiconductor spaser operating near 1.5 μm," Opt. Express 19(9), 8954-8961 (2011).

[36] Quinten, M., Leitner, A., Krenn, J. R. and Aussenegg, F. R., "Electromagnetic energy transport via linear chains of silver nanoparticles," Opt. Lett. 23(17), 1331-1333 (1998).

[37] Zabkov, I. V., Klimov, V. V., Treshin, I. V. and Glazov, O. A., "Plasmon oscillations in a linear cluster of spherical nanoparticles," Quantum Electronics 41(8), 742-747 (2011).

[38] Brongersma, M. L., Hartman, J. W. and Atwater, H. A., "Electromagnetic energy transfer and switching in nanoparticle chain arrays below the diffraction limit," Phys. Rev. B 62(R163356 (2000).

[39] Maier, S. A., [Plasmonics: Fundamentals and Applications], Springer, New York (2007).

[40] Scott, A., [Nonlinear science], Oxford University Press, Oxford (2003).